Check for updates

Effects of diamine isomers on the properties of colorless and transparent copoly(amide imide)s†

Moon Young Choi,[a] Seon Ju Lee,[a] Lee Ku Kwac,[ab] Hong Gun Kim[ab] and Jin-Hae Chang [ID] *[b]

To fully understand the structure–property relationship of aromatic copoly(amide-imide)s (Co-PAIs) and determine which factors lead to chain rigidity, we prepared two series of Co-PAIs. They were synthesized from two types of amine monomers containing *m*- and *p*-isomers and different ratios of 4,4′-(hexafluoroiso-propylidene)diphthalic anhydride (6FDA) and 4,4′-biphthalic anhydride (BPA). *m*-Substituted and *p*-substituted N,N′-[2,2′-bis(trifluoromethyl)-4,4′-biphenylene]bis(aminobenzamide) (MPAB) diamine isomers were synthesized from 3- and 4-nitrobenzoyl chloride and 2,2′-bis(trifluoromethyl) benzidine (TFB), respectively. The Co-PAI films were synthesized from poly(amic acid) (PAA), *via* solution-casting, followed by thermal imidizations. The thermal- and mechanical-properties and optical transparency of the Co-PAI films with different BPA monomer contents were investigated. We also investigated the effects of the different MPAB isomers on the Co-PAI structures. Compared with the *m*-substituted MPAB Co-PAI films, the *p*-substituted MPAB Co-PAI films have superior thermo-mechanical properties at the same monomer content. However, the optical transparencies of the *m*-MPAB Co-PAIs are slightly better than those of the *p*-MPAB Co-PAIs.

1. Introduction

Aromatic polyimides (PIs) are high-performance polymeric materials with outstanding properties, and have been evaluated for use in military applications, microelectronics, and aerospace.[1–4] PI derivatives are also one of the most important super engineering materials due to their excellent mechanical properties at high temperatures, owing to their thermal stability.[5,6] Many researchers have tried to develop high-performance PI materials with excellent optical transparency and thermo-mechanical properties.[7–9] Generally, PIs are prepared using a two-step process.[10,11] Firstly, poly(amic acid) (PAA) is spin-coated or cast on a substrate, and then converted into the corresponding PI by thermal or chemical imidization.[12–14] The molecular chains orient themselves in the plane of the film by the effect of substrate confinement. The orientation in this in-plane has a great influence on the thermo-mechanical properties and optical transparency that ultimately determine the reliability of microelectronic materials. A majority of earlier studies focused on the factors that affect the thermo-mechanical properties and optical transparencies of PIs, such as the curing conditions, imidization temperature, monomer content, *etc.*[15,16]

Rod-like PIs exhibit better in-plane orientation and improved properties, compared with kinked PIs.[17,18] This effect is most pronounced in PI films containing *p*-isomers, and is relatively insignificant in those containing *m*-isomer-type monomers.[19] The results demonstrated that the chain rigidity plays a very important role in molecular in-plane orientation. Higher chain rigidity leads to improved thermo-mechanical properties. On the other hand, replacing PI with a copolyimide (Co-PI) such as poly(amide imide) (PAI) can be a good method to overcome the difficult processability of the PI film.

In practice, however, most PAIs cannot be easily processed and used due to their excellent thermal properties and low solubility in most common solvents. Therefore, many studies have been conducted to solve such problems in processing.[20–22] These studies involved the introduction of non-coplanar structures, bulk side groups, flexible alkyl groups into the polymer main chain, and *ortho*- or *meta*-linked structures.

Generally, one of the methods for increasing the solubility and optical transparency of copoly(amide-imide) (Co-PAI) film without deteriorating high thermal property is the introduction of bulky side groups. In particular, colorless and transparent Co-PAIs have been prepared using diamine and dianhydride monomers, the bulky side groups of which contain substituted fluorine moieties (–CF₃). 2,2′-Bis(trifluoromethyl)benzidine (TFB)- and 4,4′-(hexafluoroiso-propylidene)diphthalic anhydride (6FDA)-based Co-PAIs have been investigated in terms of their thermal stabilities and optical properties.[23–25]

In order to synthesize colorless and transparent PI, a copolyimide (Co-PI) that can maintain the overall properties of PI

[a]Graduate School of Carbon Convergence Engineering, Jeonju University, Jeonju 55069, Korea

[b]Institute of Carbon Technology, Jeonju University, Jeonju 55069, Korea. E-mail: changjinhae@hanmail.net

while maintaining transparency has been studied. From the results already published by several researchers, TFB used for Co-PI has been proven as an excellent monomer that can maintain excellent thermal properties while exhibiting colorless and transparent properties.[26–29]

The introduction of bulky side groups such as $-CF_3$ makes it difficult to packing between the chains, preventing intra-molecular interactions between polymer chains. Several publications have shown that the introduction of bulky side groups to Co-PAI improves solubility and increases optical transparency.[30,31] Hasegawa *et al.*[32] reported new colorless PI based on TFB containing $-CF_3$ side group. This film shows potential applications as practically useful base materials in display devices. Earlier studies suggested that the properties of Co-PAIs depend not only on the packing coefficient and chain orientation but also on the main chain structure.[20,21]

In fact, since PAI incorporates the advantages of both polyimides and polyamides, it can exhibit a balance of desirable properties. This means that by including an amide group in the polyimide main chain, processability, solubility and moldability can be increased while maintaining thermal and mechanical properties. This means that desired thermal stability and processability can be obtained by adjusting the ratio of imide- and amide-group included in PAI.[33–36] In this study, *m*- and *p*-substituted MPAB diamine isomers were synthesized from 3- and 4-nitrobenzoyl chloride and TFB, respectively, and copolymerized with 6FDA and 4,4′-biphthalic anhydride (BPA) to produce Co-PAIs. The effects of Co-PAI composition on the thermo-mechanical properties and optical transparency were investigated. Co-PAIs with a third monomer may exhibit new properties that are not observed in homopolyimides. The physical properties of the two Co-PAI series obtained using *m*- and *p*-substituted MPAB isomers showed different properties. Furthermore, we compared the thermo-mechanical properties and optical transparencies of the two Co-PAI series.

2. Experimental method

2.1 Materials

All reagents used as monomers and solvents were purchased from Aldrich Chemical Co. (Yongin, Korea) and TCI (Tokyo, Japan). All purchased reagents were used without purification.

2.2 Preparation of diamine monomers

The *m*- and *p*-substituted MPABs were synthesized *via* a multiple-step route. The amine, *p*-MPAB, which has the amide group used in this experiment, was synthesized directly in the laboratory. Firstly, 5 g TFB (1.56×10^{-2} mol) and 150 mL THF were added to a 250 mL round flask and mixed until the mixture completely soluble. 5.80 g 4-nitrobenzoyl chloride (3.13×10^{-2} mol) and 150 mL THF were added to a 250 mL beaker, mixed violently, and slowly dropped into the TFB solution. 10 mL pyridine was added as a catalyst and mixed at 25 °C for 6 h in N_2 conditions. The sediment from the finished solution was simply filtered, and the powder obtained was washed with 2 L distilled water. After repeating this process twice, it was washed with

distilled water and ethanol (v/v = 8/2) to prepare purified powder. The obtained powder was vacuum-dried for 12 h in a 100 °C vacuum oven. 8 g of the dried powder (1.29×10^{-2} mol) was taken in a 500 mL round flask, and 400 mL ethanol was added to completely dissolve the powder at 60 °C; then, 0.14 g palladium/charcoal (Pd/C) and 5.96 mL hydrazine monohydrate were added and mixed for 12 h to induce hydrogenation. After completion of the hydrogenation reaction, the Pd/C catalyst was filtered out and the product was precipitated in 2 L distilled water, followed by drying in a 100 °C vacuum oven for 12 h. The product yield of the white powder was 79%. The overall process of *m*-/*p*-MPAB synthesis is shown in Scheme 1. Anal. calcd for $C_{28}H_{20}O_2N_4F_6$ ($M_w = 558.50$): C = 60.22%, H = 3.61%, N = 10.03%. Found: C = 60.18%, H = 3.57%, N = 10.08% for *p*-MPAB and C = 60.20%, H = 3.59%, N = 10.10% for *m*-MPAB.

2.3 Preparation of Co-PAI films

The monomer contents of the Co-PAIs are shown in Table 1. The synthesis procedures for the Co-PAI films were the same for all the monomer compositions used; the preparation of sample B (MPAB : 6FDA : BPA mole ratio = 1 : 0.9 : 0.1) is detailed herein as a representative example. MPAB (2.02 g, 3.62×10^{-3} mol) and BPA (0.11 g, 3.62×10^{-4} mol) were added to 40 mL of DMAc, and then this mixture was stirred at 0 °C for 30 min to produce a homogeneous solution. In a separate beaker, 6FDA (1.45 g, 3.26×10^{-3} mol) was dissolved in 20 mL of DMAc and the obtained solution was added to the MPAB/BPA/DMAc system, with vigorous stirring, to obtain a homogeneous solution of DMAc and PAA with an 18 wt% solid content.

Pyridine (0.79 g, 7.76×10^{-3} mol) and acetic anhydride (1.85 g, 1.81×10^{-2} mol) were added to complete the chemical imidization of the PAA solution. This solution was stirred at 25 °C for 1 h, and then at 80 °C for 2 h, under N_2 flow. Methanol (2 L) was added to the solution to precipitate solid Co-PAI. The filtered Co-PAI precipitate was dried *in vacuo* at 100 °C for 12 h. In a separate beaker, the precipitate was dissolved by vigorous stirring in DMAc (60 mL). This solution was cast onto glass plates (10 cm × 10 cm) and then stabilized under an air atmosphere at 50 °C for 1 h with N_2 flow. For solvent removal,
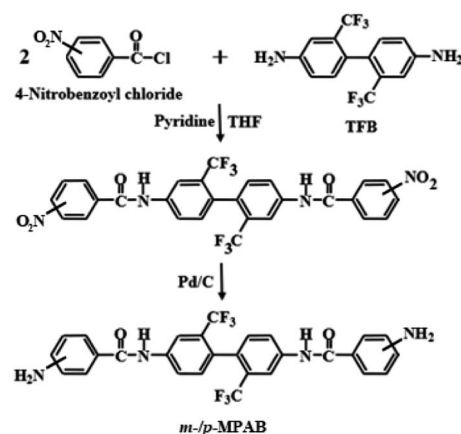
Scheme 1 Synthesis route to *m*-/*p*-MPAB.

Table 1 Monomer compositions in Co-PAIs

| Co-PAI	m-/p-MPAB (mole)	6FDA (mole)	BPA (mole)	Molar ratio
A	1.0	1.0	0	1 : 1 : 0
B	1.0	0.9	0.1	1 : 0.9 : 0.1
C	1.0	0.8	0.2	1 : 0.8 : 0.2
D	1.0	0.7	0.3	1 : 0.7 : 0.3
E	1.0	0.6	0.4	1 : 0.6 : 0.4

the film was dried *in vacuo* at 70 °C for 1 h. The resulting film was heat-treated at various temperatures (100, 130, 160, 190, 220, and 250 °C) for 30 min each, to promote imidization. The film was soaked in hot water and stripped from the glass. The film thickness was approximately 34–36 μm. Scheme 2 shows the synthesis route to Co-PAI.

We tried to synthesize a Co-PAI film containing more than 0.4 mol BPA. However, repeated attempts to polymerize the Co-PAI film containing 0.5 mol BPA failed due to brittleness during the film fabrication process. All the obtained Co-PIs were mixed with various solvents and observed for a long time, but they were not completely soluble, and hence, solution viscosity measurement failed.

2.4 Characterization

The structure of the synthesized material was identified by Fourier-transform infrared (FT-IR) spectroscopy (Bruker VERTEX 80v, Berlin, Germany). The ^1H NMR spectra were confirmed with a Bruker DPX 200 MHz NMR spectrometer (Berlin, Germany) and were referenced to tetramethylsilane (TMS). Elemental analyses were carried out in a PerkinElmer Model 2400 CHNS/O analyzer.

Differential scanning calorimeter (DSC; NETZSCH 404 F3 Pegasus®), thermogravimetric analyzer (TGA; TA Q500), and thermomechanical analyzer (TMA-2940) were used in the same conditions as the previously published papers.[37,38] In particular, TMA was measured in the range of 30–230 °C. For the tensile properties of the film, a universal testing machine (UTM, Instron model 5564) was used, and the size of the film was 5 mm × 70 mm.
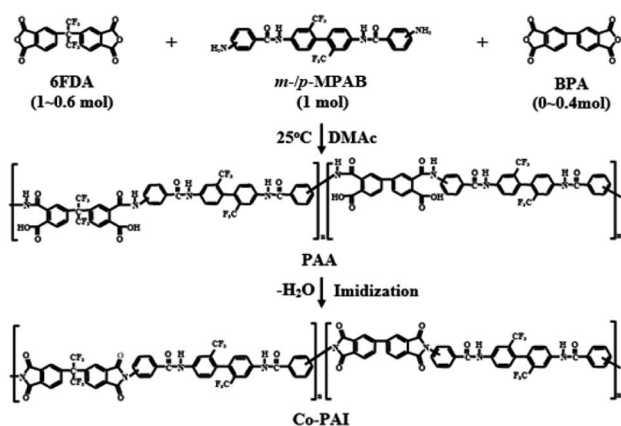
The color intensity of the Co-PAI film obtained according to the BPA molar ratio was measured with a Minolta spectrophotometer (CM-3500d). Yellow index (YI) measurements of the films were carried out at an observational angle of 10°, using a CIE-D illuminant. A Shimadzu UV-3600 spectrophotometer was used to obtain the UV-vis value of the film.

3. Results and discussion

3.1 Monomer analysis by FT-IR and ^1H-NMR

The structure of the synthesized *p*-MPAB monomer was confirmed using FT-IR and ^1H-NMR spectra. NH_2 stretching peaks were observed at 3507 and 3298 cm^{-1}, respectively, and N–H peak was confirmed at 3411 cm^{-1}. The C=O stretching peak was seen at 1654 cm^{-1}, the aromatic C=C peaks were observed at 1600–1450 cm^{-1}, and the C–N peak was seen at 1294 cm^{-1}.[39] From the results of the ^1H-NMR spectrum, a proton peak of N–H was shown at 10.2 ppm (2H), and peaks of protons of aromatic rings appeared at 6.7 to 8.3 ppm (14H). The proton peak of the amine group was confirmed at 5.8 ppm (4H).[39] Through the FT-IR and ^1H-NMR spectrum results, it was confirmed that the chemical structure of *p*-MPAB was successfully synthesized. *m*-MPAB was also confirmed in the same way.

3.2 Polymer analysis by FT-IR

FT-IR spectra were used to confirm the formation of Co-PAA and Co-PAI from PAA; the spectra of Co-PAA and the Co-PAI (sample B) are shown in Fig. 1. In Co-PAA, the C=O stretching peak of the acid at 1700 cm^{-1} and the stretching peak of amide at 1602 cm^{-1} were observed, respectively. In Co-PAI, the peak shifted to a slightly higher frequency, and C=O peaks were observed at 1782 cm^{-1} (in phase) and 1712 cm^{-1} (out of phase), respectively. In addition, a peak corresponding to C–N–C stretching indicating the presence of imide was observed at 1378 cm^{-1}.[39]

3.3 Thermal behavior

Comparative DSC results for the Co-PAI films containing *m*- and *p*-MPABs are listed in Table 2. The glass transition temperature (T_g) values of the Co-PAI films increased gradually from 263 to
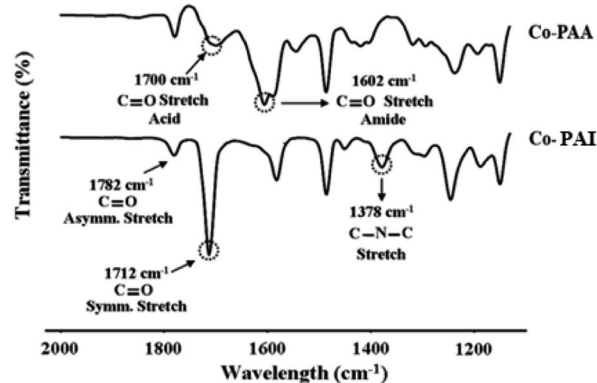

Scheme 2 Synthesis route to Co-PAI.

Fig. 1 FT-IR spectra of Co-PAA and Co-PAI (sample B).

Table 2 Thermal properties of Co-PAI films

	m-MPAB				p-MPAB			
Co-PAI	T_g (°C)	$T_D^{i\,a}$ (°C)	wt_R^{600b} (%)	CTE^c (ppm °C^{-1})	T_g (°C)	T_D^i (°C)	wt_R^{600} (%)	CTE (ppm °C^{-1})
A	263	438	62	62.6	343	448	64	31.8
B	266	439	66	52.4	347	454	69	30.6
C	268	437	65	47.7	349	455	68	27.2
D	271	442	67	46.9	351	449	68	24.9
E	273	442	67	46.2	—	451	69	22.7

^{a} At a 2% initial weight-loss temperature. ^{b} Weight percent of the residue at 600 °C. ^{c} Coefficient of thermal expansion obtained in the second heating cycle between 50 and 220 °C.

273 °C for m-TFAB and from 343 to 351 °C for p-MPAB, with an increase in BPA loading (from 0 to 0.4 mol). This increase in T_g was likely due to two factors:[40,41] (1) the significant effect of rigid rod-like monomer structures on the free volume of the polymer, and (2) the confinement of inter-reacted polymer chains within the copolymers, which prevents the segmental motion of the chains. It is generally accepted that the introduction of BPA into a polymer structure improves the thermal properties, since the BPA monomer is thermally stable. This might be because BPA monomers with high chain stiffness have a greater effect on T_g than 6FDA.[42,43] The DSC thermograms of the m- and p-Co-PAI films with different BPA mole ratios are shown in Fig. 2.

Comparative TGA results for the Co-PAI films are shown in Table 2. The initial thermal degradation temperature (T_D^i) showed a trend different from that of the T_g. In our investigation, the T_D^is of the Co-PAI films, determined at 2% weight loss, were found to be virtually independent of the BPA content, within the error range. This result suggests that the

thermal stabilities are independent of the amount of BPA incorporated into the Co-PAI films. Specifically, the T_D^i values ranged from 437 to 442 °C for the m-MPAB samples and from 448 to 455 °C for the p-MPAB samples, as BPA content increased from 0 to 0.4 mol. The weight of the residue at 600 °C (wt_R^{600}) was found to be virtually constant with increase in BPA loading from 0 to 0.4 mol, ranging from 62 to 67% for m-MPAB Co-PAIs and from 64 to 69% for p-MPAB Co-PAIs. However, compared with the m-MPAB Co-PAI films, the p-MPAB Co-PAI films have superior thermal stabilities (T_D^i and wt_R^{600}) at the same monomer composition. After all, the thermal stability of a polymer is closely related to the rigidity of the chain and the molecular packing of the polymer chain. The rigid linear structure also associated with p-linked amines appears to support the delicate intermolecular interactions that promote thermal stability in this Co-PAI system.[44,45]

3.4 Coefficient of thermal expansion

The stiffness of the main polymer chain is governed by the rod-like monomer structure, and this stiffness affects the physical properties such as the CTE, and in-plane orientation.[46,47] Different CTE values may be attributed to differences in the higher order structure of the films. The CTE values for the Co-PAIs, over the temperature range of 50–200 °C, are also listed in Table 2. The CTE values of the Co-PAI films decreased with an increase in BPA loading up to 0.4 mol. For example, the CTEs of the Co-PAI films containing m-MPAB decreased gradually from 62.6 to 46.2 ppm °C^{-1} when the BPA loading was increased from 0 to 0.4 mol, indicating that the magnitude of the reduction in thermal expansion because of BPA depended on the Co-PAI molecular orientation and the rigid nature of the BPA monomer. A similar behavior was observed for the p-substituted MPAB Co-PAI films; the CTE values decreased gradually from 31.8 to 22.7 ppm °C^{-1} for the same BPA monomer loading. The above results also indicate that the CTE values of the p-MPAB Co-PAI films are much superior to those of the m-MPAB Co-PAI films.

Upon heating, the in-plane-oriented Co-PAI molecules tended to relax in a direction normal to their original direction, and therefore expanded mainly in the out-of-plane direction.[17–19] Co-PAIs containing BPA monomers were more rigid than polymers containing 6FDA, so they were not easily deformed or relaxed. Consequently, the BPA monomers effectively restricted the thermal expansion of the Co-PAI molecules in the out-of-plane direction. The CTEs for the Co-PAI films with different BPA
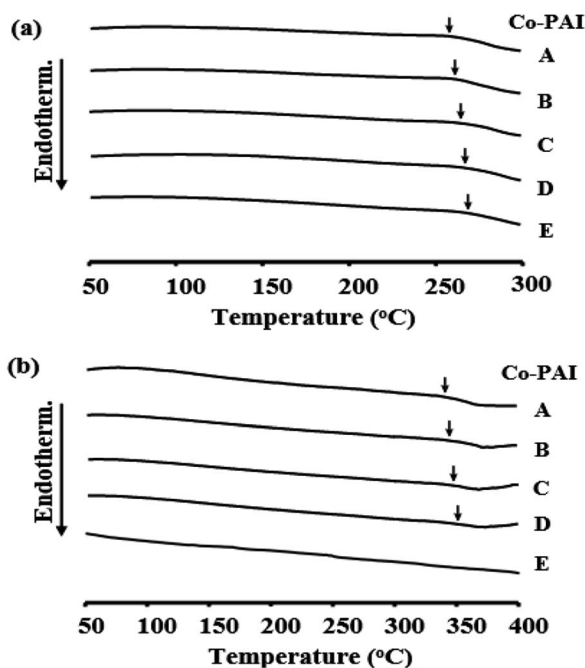

Fig. 2 DSC thermograms of Co-PAI films containing (a) m-MPAB and (b) p-MPAB.
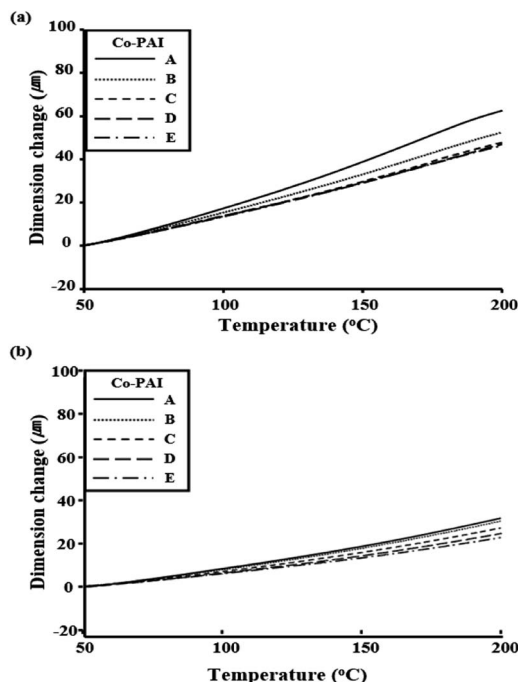
Fig. 3   TMA thermograms of Co-PAI films containing *m*-MPAB and (b) *p*-MPAB.

Fig. 4   3-Dimensional chemical structures of Co-PAIs containing (a) *m*-MPAB and (b) *p*-MPAB.
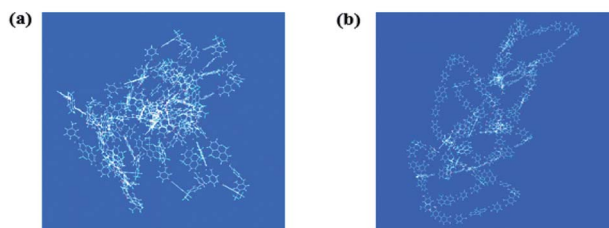
monomer contents, obtained using the TMA, are shown in Fig. 3. The *p*-MPAB skeleton of the low-thermal-expansion Co-PAIs is composed of a benzene ring with an amide functional group fused at the *para*-position. In contrast, Co-PAIs incorporating a bent structure, such as a benzene ring fused at the *meta*-position, normally have high CTEs. This indicates that the CTE may be closely related to the cross-packing of the molecular structure.[48,49]

The 3-dimensional (3-D) structures from two isomers are depicted in Fig. 6, along with the optimized linear structures of the *m*- and *p*-MPAB monomers. Compared to the *m*-MPAB species, the *p*-MPAB structure is more rigid and rod-like regardless of the BPA monomer content in the Co-PAI polymer chains, presumably to maximize the linearity of the polymer chains (see Fig. 4(b) in compositions C and E).

3.5   Mechanical properties

Table 3 shows that the overall mechanical properties of the Co-PAI films were virtually constant as the BPA content increased
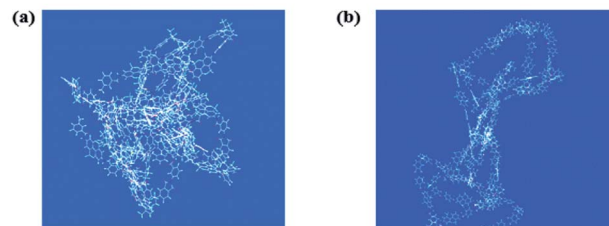
from 0 to 0.4 mol. In the case of *m*-MPAB, the ultimate strength and initial modulus were virtually constant, increasing only from 133 to 137 MPa and from 3.83 to 3.91 GPa, respectively (see Table 3), with increase in the BPA loading from 0 to 0.4 mol. Similarly, in the case of *p*-MPAB, the ultimate strength and initial modulus did not change significantly, varying only from 149 to 153 MPa and 4.63 to 4.96 GPa, respectively, for the same BPA loadings. The elongation at breakage (EB) of the Co-PAI films was found to be almost constant with variation in the BPA mole ratio, *i.e.*, it varied from 6 to 9% and from 15 to 23% for *m*- and *p*-MPAB, respectively, as the BPA content was increased from 0 to 0.4 mol. Analogous to the results for thermal behavior, the values of the mechanical properties were found to be virtually unchanged for variations in BPA monomer contents in the Co-PAI films.

The mechanical tensile properties of the Co-PAI films synthesized with *p*-MPAB are superior to those of the Co-PAI films containing *m*-MPAB diamine, for all the BPA contents. The effects of *p*-MPAB on the mechanical properties of the Co-PAIs are similar to those on the thermal properties and CTEs, and are principally caused by the rigid-rod-type structure of the Co-PAI with *p*-MPAB as shown in Fig. 4.

Table 3   Mechanical properties of Co-PAI films

Co-PAI	*m*-MPAB			*p*-MPAB		
	Ult. str. (MPa)	Ini. mod. (GPa)	E.B.[a] (%)	Ult. str. (MPa)	Ini. mod. (GPa)	E.B. (%)
A	137	3.88	7	151	4.63	23
B	136	3.88	9	152	4.87	17
C	136	3.83	6	153	4.87	15
D	133	3.91	6	149	4.96	22
E	133	3.85	8	150	4.85	15

[a] Elongation percentage at break.

Table 4 Optical properties of Co–PAI films

	m-MPAB				p-MPAB			
Co-PAI	Thickness (μm)	$\lambda_o{}^a$ (nm)	550 nm^{trans} (%)	YI^b	Thickness (μm)	λ_o (nm)	550 nm^{trans} (%)	YI
A	35	357	88	1.6	35	355	88	1.9
B	34	369	88	2.0	35	369	87	2.2
C	36	369	89	2.0	35	380	87	2.3
D	35	373	88	2.8	36	382	88	3.4
E	34	376	88	4.1	34	386	88	4.6

^{a} Cut-off wavelength. ^{b} Yellow index.

3.6 Optical transparency

Several approaches have been used to prepare transparent and colorless PIs, such as introducing a curved structure in the main chain to reduce linearity, bulk substituents in the main chain to reduce intermolecular packing, and the introduction of strong electron-withdrawing elements such as fluorine.[50,51]

In general, the introduction of –CF$_3$ groups, which are very strong electron withdrawing groups, can improve the optical properties of polymers. In addition, the introduction of bulky side groups will reduce the packing density between polymer chains, further reducing intermolecular interactions between polymer chains. Ultimately, these factors increase the optical transparency of the PAI film.[25,52,53]

The optical properties of the Co–PAIs with different BPA contents are summarized in Table 4. The color intensities of the films can be explained using the λ_o values observed in the UV-vis absorption spectra. The UV-vis spectra of the Co–PAI films with BPA mole ratios ranging from 0 to 0.4 mol are shown in Fig. 5. All the Co–PAI films exhibited λ_os shorter than 400 nm. The λ_o increased linearly with an increase in BPA content to 0.4 mol, due to the CT complex of the rigid rod-like BPA monomer structure (see Table 4). The most lightly colored pure PAIs correspondingly exhibited shorter λ_o values, because the –CF$_3$ groups in the monomers significantly reduced the intermolecular interactions and inhibited the formation of a CT complex.[29] The superior transparency of these CF$_3$-group-based PAIs may be due to the limited electronic conjugation along their polymer main chains. The transmittances of the m- and p-MPAB Co–PAI films, at 550 nm, indicate excellent optical transparency, as shown in Table 4. These colorless and transparent Co–PAI films had maximum UV transmittances of greater than 85% at 550 nm, and exhibited excellent optical properties.

Additionally, the color intensity of the Co–PAI films was affected by the BPA monomer content (Table 4). The Co–PAI films with a lower BPA content exhibited lower YI values than
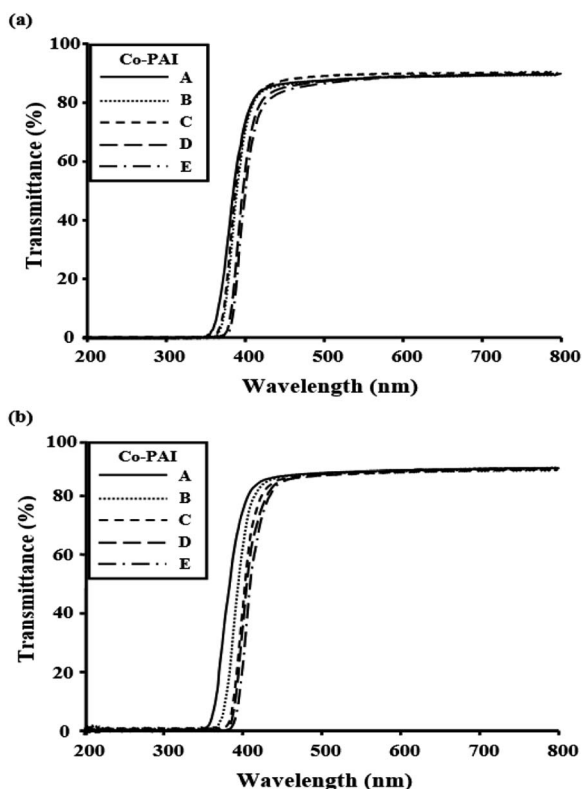

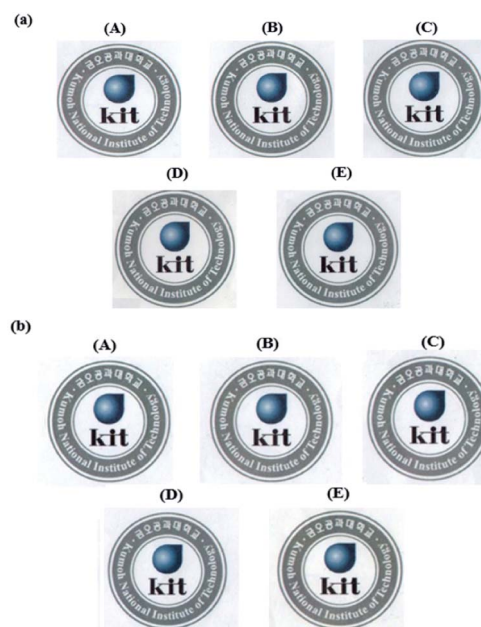**Fig. 5** UV-vis transmittance (%) of Co–PAI films containing (a) m-MPAB and (b) p-MPAB.

Fig. 6 Photographs of Co–PAI films containing (a) m-MPAB and (b) p-MPAB.

the corresponding Co-PAIs with a higher BPA content. However, the magnitude of these changes was not significant. The YI values of the homo PAIs with *m*- and *p*-MPABs were 1.6 and 1.9, respectively. When the BPA loading was initially increased to 0.1 mol and then to 0.4 mol, the YI value increased from 2.0 to 4.1 in the case of *m*-MPAB and from 2.2 to 4.6 in the case of *p*-MPAB. In contrast to the thermo-mechanical properties, the optical transparencies of the *m*-MPAB Co-PAIs are slightly better than those of the *p*-MPAB Co-PAIs. The *m*-MPAB in Co-PAIs has a bent structure, which inhibits the CT complex formation and intermolecular interactions observed in *p*-MPAB Co-PAIs, resulting in superior optical transparencies.

All the solvent-cast hybrid films with BPA monomer contents in the range of 0–0.4 mol were almost colorless, as shown in Fig. 6. However, their optical transparencies decreased slightly when the BPA content increased. The Co-PAI film containing 0.4 mol BPA was slightly cloudier than the films containing 0.1–0.3 mol BPA, but the optical transparency was still good, as it was possible to read a letter through the film. The levels of transparency were not significantly affected by the increase in the BPA monomer content, as shown in Fig. 6.

4. Conclusions

This study focused on the synthesis of Co-PAI films from PAA, *via* solution-casting, using chemical and thermal imidizations. Co-PAI films were synthesized from *m*- and *p*-MPAB and 6FDA, with different BPA mole ratios. The BPA content of the Co-PAI films was varied from 0 to 0.4 mol, and the effects on the thermo-mechanical properties and optical transparencies of the films were examined. It was found that with an increase in BPA content (from 0 to 0.4 mol), the T_g and CTE values of the Co-PAI films improved gradually, whereas the optical transparency of the Co-PAI films deteriorated. The thermal stability and mechanical properties were found to be virtually unchanged with a variation in BPA monomer contents in the Co-PAI films.

We also examined the effects of the two different types of MPAB amine monomers on the Co-PAI film structures. By comparing the results for the two tested MPABs, we found that the addition of *p*-MPAB was more effective than that of *m*-MPAB with regard to improving the thermo-mechanical properties, whereas the addition of *m*-MPAB was more effective than that of *p*-MPAB with regard to improving the optical transparency of the Co-PAI films.

Depending on the optical transparency, the PAI film studied in this paper can be used in flexible sun protection devices, flexible display polymer films, alignment films for liquid crystal displays, and optical plates for flat light wave circuits.

Conflicts of interest

There are no conflicts to declare.

Acknowledgements

References

1 Y. H. Yu, J. M. Yeh, S. J. Liou, C. L. Chen, D. J. Liaw and H. Y. Lu, *J. Appl. Polym. Sci.*, 2004, **92**, 3573.

2 J. W. Park, M. Lee, M.-H. Lee, J. W. Liu, S. D. Kim, J. Y. Chang and S. B. Rhee, *Macromolecules*, 1994, **27**, 3459.

3 C. Y. Yang, S. L. C. Hsu and J. S. Chen, *J. Appl. Polym. Sci.*, 2005, **98**, 2064.

4 H.-W. Wang, R.-X. Dong, H.-C. Chu, K.-C. Chang and W.-C. Lee, *Mater. Chem. Phys.*, 2005, **94**, 42.

5 M. B. Saeed and M.-S. Zhan, *Eur. Polym. J.*, 2006, **42**, 1844.

6 H. Wei, X. Fang, Y. Han, B. Hu and Q. Yan, *Eur. Polym. J.*, 2010, **46**, 246.

7 X. Zhao, Y. Guan, D. Wang, G. Song, G. Dang, C. Chen and H. Zhou, *Polymer*, 2014, **55**, 3634.

8 R. A. Dine-Hart and W. W. Wright, *Macromol. Chem.*, 1971, **143**, 189.

9 Y. S. Jung, S. J. Byun, S. J. Park and H. M. Lee, *ACS Appl. Mater. Interfaces*, 2014, **6**, 6054.

10 I. H. Choi and J.-H. Chang, *Polymer*, 2010, **34**, 480.

11 X. Wang, Y.-F. Li, T. Ma, S. Zhang and C. Gong, *Polymer*, 2006, **47**, 3774.

12 H.-S. Jin, J.-H. Chang and J.-C. Kim, *Macromol. Res.*, 2008, **16**, 503.

13 M. Hasegawa, T. Matano, Y. Shindo and T. Sugimura, *Macromolecules*, 1996, **29**, 7897.

14 C.-P. Yang, Y.-Y. Su and Y.-C. Chen, *Eur. Polym. J.*, 2006, **42**, 721.

15 I. H. Choi and J.-H. Chang, *Polymer*, 2010, **34**, 391.

16 R. A. Dine-Hart and W. W. Wright, *J. Appl. Polym. Sci.*, 1967, **11**, 609.

17 R. M. Ikeda, *J. Polym. Sci., Part B: Polym. Lett.*, 1966, **4**, 353.

18 M. T. Pottiger, J. C. Coburn and J. R. Edman, *J. Polym. Sci., Part B: Polym. Phys.*, 1994, **32**, 825.

19 T. Dingemans, E. Mendes, J. J. Hinkley, E. S. Weiser and T. L. StClair, *Macromolecules*, 2008, **41**, 2474.

20 W. Li, X. Qian, H. Shi, W. Zhou, Y. Cai, Y. Liu and K. Shen, *J. Polym. Sci., Part A: Polym. Chem.*, 2017, **55**, 3243.

21 K. Kim, T. Yoo, J. Lee, M. Kim, S. Lee, G. Kim, J. Kim, P. Han and H. Han, *Prog. Org. Coat.*, 2017, **112**, 37.

22 A. Sarkar, P. N. Honkhambe, C. V. Avadhani and P. P. Wadgaonkar, *Eur. Polym. J.*, 2007, **43**, 3646.

23 Y. Liu, X. Qian, H. Shi, W. Zhou, Y. Cai and W. Li, *Eur. Polym. J.*, 2017, **94**, 392.

24 M.-D. Damaceanu, C.-P. Constantin, A. Nicolescu, M. Bruma, N. Belomoina and R. S. Begunov, *Eur. Polym. J.*, 2014, **50**, 200.

25 P. K. Tapaswi and C.-S. Ha, *Macromol. Chem. Phys.*, 2019, **220**, 1800313.

26 T. Matsuura, Y. Hasuda, S. Nishi and N. Yamada, *Macromolecules*, 1991, **24**, 5001.

27 T. Matsuura, M. Ishizawa, Y. Hasuda and S. Nishi, *Macromolecules*, 1992, **25**, 3540.

28 T. Matsuura, N. Yamada, S. Nishi and Y. Hasuda, *Macromolecules*, 1993, **26**, 419.

29 T. Matsuura, S. Ando, S. Sasaki and F. Yamamoto, *Macromolecules*, 1994, **27**, 6665.

30 H.-J. Ni, J.-G. Liu, Z.-H. Wang and S.-Y. Yang, *J. Ind. Eng. Chem.*, 2015, **28**, 16.

31 W. J. Bae, M. K. Kovalev, F. Kalinina, M. Kim and C. Cho, *Polymer*, 2016, **105**, 124.

32 M. Hasegawa, Y. Watanabe, S. Tsukuda and J. Ishii, *Polym. Int.*, 2016, **65**, 1063.

33 H. Behniafar and S. Mohammadparast-delshaad, *Polym. Degrad. Stab.*, 2012, **97**, 228.

34 Y. Kobayashi, Y. Fujiwara, T. Kitaoka, Y. Oishi and Y. Shibasaki, *React. Funct. Polym.*, 2016, **108**, 78.

35 H. Behniafar and A. Abedini-pozveh, *Polym. Degrad. Stab.*, 2011, **96**, 1327.

36 B. Lee, S. D. Kim, J. Park, T. Byun, S. J. Kim, M. Seo and S. Y. Kim, *J. Polym. Sci., Part A: Polym. Chem.*, 2018, **56**, 1782.

37 J. Ju and J.-H. Chang, *Polymer*, 2015, **39**, 275.

38 J. Ju and J.-H. Chang, *J. Thermoplast. Compos. Mater.*, 2016, **29**, 558.

39 D. L. Pavia, G. M. Lampman and G. S. Kriz, *Introduction to spectroscopy*, Cengage Learning, Boston, MA, USA, 2008.

40 J. P. Fernandez-Blazquez, A. Bello and E. Perez, *Macromolecules*, 2004, **37**, 9018.

41 B. J. Ash, L. S. Schadler and R. W. Siegel, *Mater. Lett.*, 2002, **55**, 83.

42 X. Hu, H. Mu, Y. Wang, Z. Wang and J. Yan, *Polymer*, 2018, **134**, 8.

43 M. Hasegawa, T. Ishigami and J. Ishii, *Polymer*, 2015, **74**, 1.

44 M. Hasegawa, T. Kaneki, M. Tsukui, N. Okubo and J. Ishii, *Polymer*, 2016, **99**, 292.

45 B.-K. Chen, Y.-T. Fang, J.-R. Cheng and S.-Y. Tsay, *J. Appl. Polym. Sci.*, 2007, **105**, 1093.

46 J. H. Petropoulos, *Polym. Membr.*, 2005, **1**, 93.

47 D. J. Chaiko and A. A Leyva, *Chem. Mater.*, 2005, **17**, 13.

48 F. E. Arnold, S. Z. D. Cheng, S. L. C. Hsu, C. J. Lee, F. W. Harris and S.-F. Lau, *Polymer*, 1992, **33**, 5179.

49 C. Guo, J. Liu, L. Yin, M. Huangfu, Y. Zhang, X. Wu and X. Zhang, *Fibers Polym.*, 2018, **19**, 1706.

50 G. Mousa, R. B. Farshad and B. Maasoomeh, *Des. Monomers Polym.*, 2014, **17**, 101.

51 L. Li, Y. Xu, J. Che, X. Su and C. Song, *Polym. Bull.*, 2018, **75**, 5777.

52 L. Luo, J. Yao, X. Wang, K. Li, J. Huang, B. Li, H. Wang, Y. Feng and X. Liu, *Polymer*, 2014, **55**, 4258.

53 B. V. Kotov, T. A. Gordina, V. S. Voishchev, O. V. Kolninov and A. N. Pravednikov, *Polym. Sci.*, 1977, **19**, 711.